

Discovery of VU6007496: Challenges in the Development of an M₁ Positive Allosteric Modulator Backup Candidate

Julie L. Engers, Katrina A. Bollinger, Rory A. Capstick, Madeline F. Long, Aaron M. Bender, Jonathan W. Dickerson, Weimin Peng, Christopher C. Presley, Hyekyung P. Cho, Alice L. Rodriguez, Colleen M. Niswender, Sean P. Moran, Zixiu Xiang, Anna L. Blobaum, Olivier Boutaud, Jerri M. Rook, Darren W. Engers, P. Jeffrey Conn, and Craig W. Lindsley*



Cite This: *ACS Chem. Neurosci.* 2024, 15, 3421–3433



Read Online

ACCESS |



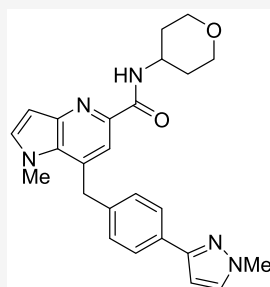
Metrics & More



Article Recommendations

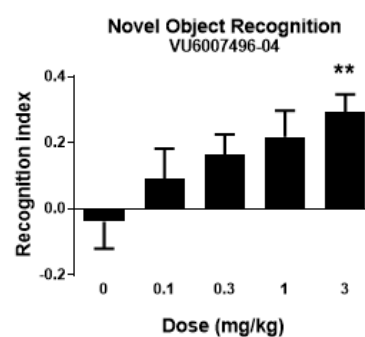


Supporting Information



VU6007496

h M₁ EC₅₀ = 228 nM, 80% ACh_{max}
h M₁ EC₅₀ (agonsim) >10 μM, 24% ACh_{max}
h M₂₋₅ EC₅₀: inactive
r M₁ EC₅₀ = 94 nM, 91% ACh_{max}
r M₁ EC₅₀ (agonsim) = 7.3 μM, 36% ACh_{max}
r M₂₋₅ EC₅₀: inactive
rat K_p = 0.42; K_{p,uu} = 0.36



ABSTRACT: Herein we report progress toward a backup clinical candidate to the M₁ positive allosteric modulator (PAM) VU319/ACP-319. Scaffold-hopping from the pyrrolo[2,3-*b*]pyridine-based M₁ PAM VU6007477 to isomeric pyrrolo[3,2-*b*]pyridine and thieno[3,2-*b*]pyridine congeners identified several backup contenders. Ultimately, VU6007496, a pyrrolo[3,2-*b*]pyridine, advanced into late stage profiling, only to be plagued with unanticipated, species-specific metabolism and active/toxic metabolites which were identified in our phenotypic seizure liability *in vivo* screen, preventing further development. However, VU6007496 proved to be a highly selective and CNS penetrant M₁ PAM, with minimal agonism, that displayed excellent multispecies IV/PO pharmacokinetics (PK), CNS penetration, no induction of long-term depression (or cholinergic toxicity) and robust efficacy in novel object recognition (minimum effective dose = 3 mg/kg p.o.). Thus, VU6007496 can serve as another valuable *in vivo* tool compound in rats and nonhuman primates, but not mouse, to study selective M₁ activation.

KEYWORDS: muscarinic acetylcholine receptor subtype 1 (M₁), positive allosteric modulator (PAM), cognition, metabolism

INTRODUCTION

The resurgence of muscarinic acetylcholine receptors (mAChRs or M₁₋₅) at the forefront of CNS drug discovery for a variety of neuropsychiatric disorders, driven by the pending FDA approval of xanomeline **1** (an M₁/M₄ agonist, combined with a peripheral muscarinic antagonist as KarXT),^{1–3} has focused attention on the development of selective M₁ and M₄ positive allosteric modulators (PAMs). While M₄ PAMs have demonstrated preclinical and clinical efficacy for treatment of the positive symptoms of schizophrenia, M₁ PAMs offer promise for treating cognitive dysfunction in schizophrenia, Alzheimer's disease and other CNS disorders.^{4–7} Potent ago-PAMs, such as 2–5 (Figure 1),^{8–12} overstimulate the M₁ receptor and lead to adverse events (AEs) and cholinergic toxicity, which has diminished enthusiasm for the mechanism. However, PAMs with minimal to no M₁ agonism, such as 6–8,^{13–16} proved devoid of AEs

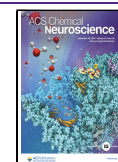
and cholinergic toxicity in preclinical animal models. Interestingly, the M₁ ago-PAM TAK-071 (**9**),^{17,18} displaying low cooperativity, was efficacious in a number of preclinical rodent models and has advanced into human clinical testing. From our efforts with VU319/ACP-319 (structure not disclosed at this time), an M₁PAM with no detectable M₁ agonism proved devoid of AEs, cholinergic toxicity, and other toxicology findings in rat, dog, and nonhuman primate to support an open IND by the FDA. Recently, safety and pharmacokinetic data from a Phase I single ascending dose

Received: August 7, 2024

Revised: August 22, 2024

Accepted: August 22, 2024

Published: August 28, 2024



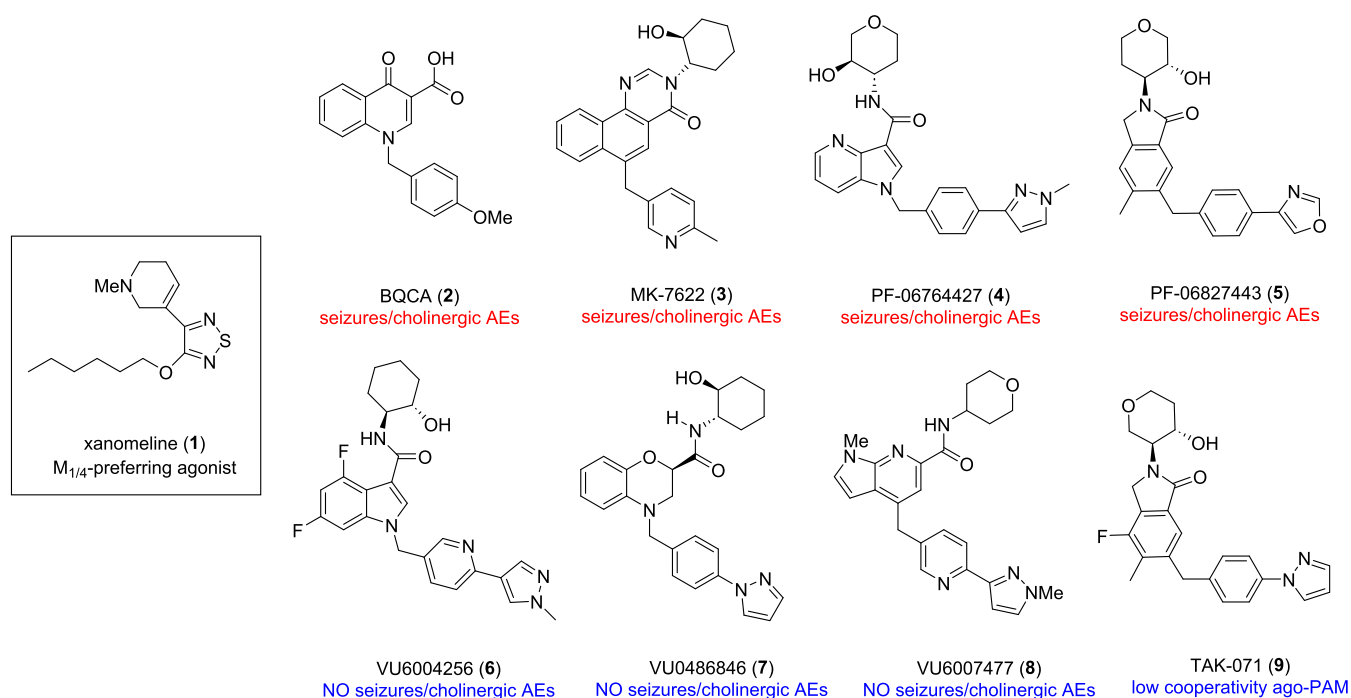


Figure 1. Structures of xanomeline (1), representative M_1 ago-PAMs with cholinergic AEs 2–5, representative “pure” PAMs devoid of M_1 agonism 6–8, and the low cooperative M_1 ago-PAM TAK-071 (9).

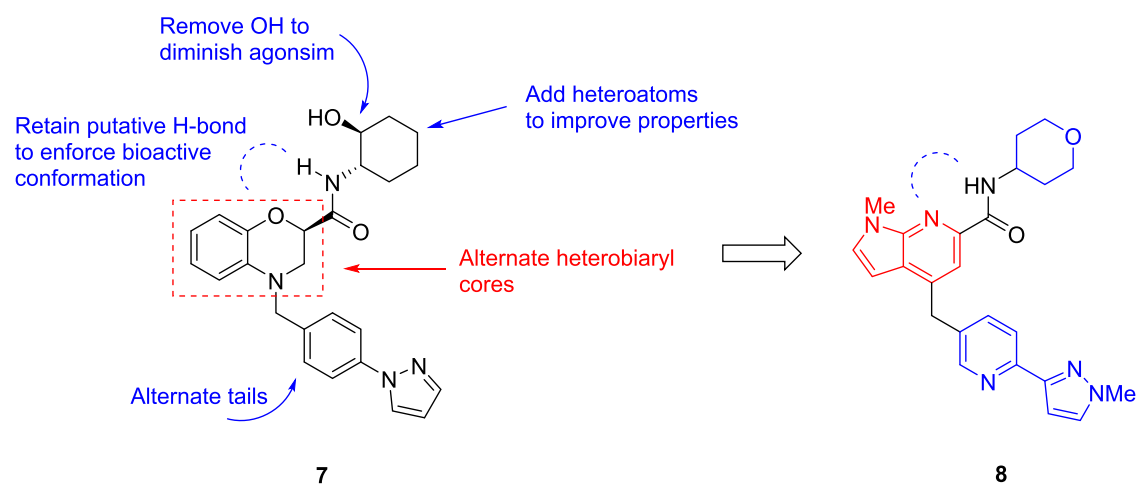


Figure 2. Initial scaffold-hopping exercise from 7 that led to 8, a novel M_1 PAM devoid of cholinergic toxicities and AEs.

(SAD) study for ACP-319 have been reported.^{19,20} This M_1 PAM was well tolerated, with no cholinergic side effects noted, at doses showing cognitive improvement and functional target engagement. Moreover, pharmacokinetic (PK) data demonstrated that ACP-319 demonstrated good absorption and bioavailability in man with a half-life supporting once daily dosing.^{19,20} Based on these data, the team was charged with developing a chemically orthogonal backup compound to ACP-319. Here, we disclose the chemical optimization of VU6007477 (8) and the challenges and tribulations that led to the discovery of not a backup clinical candidate, but a new *in vivo* tool compound, VU6007496.

RESULTS AND DISCUSSION

Design. Our initial backup campaign focused on the chemically orthogonal M_1 PAM scaffold 7 (VU0486846), devoid of M_1 agonism, AEs, and cholinergic toxicity, but which

exhibited an unacceptable CYP₄₅₀ profile.¹⁵ We elected to employ a scaffold-hopping approach to replace the benzomorfoline core while surveying alternate amides (deleting the agonism-prone hydroxyl moiety and incorporating heteroatoms) and various southern tail moieties (Figure 2). This exercise led to exceedingly steep structure–activity relationship (SAR) in terms of the generation of M_1 ago-PAMs (displaying cholinergic side effects) *versus* M_1 PAMs with minimal to no M_1 agonism, with a single analog advancing as a new M_1 PAM *in vivo* tool compound, 8 (VU6007477), with robust precognitive efficacy and no cholinergic toxicity or AEs.¹⁶ However, the overall profile of 8 did not warrant advancement as a backup candidate to VU-319/ACP-319.

Far more dramatic departures in subsequent scaffold-hopping campaigns were met with resolute failure to provide M_1 PAMs devoid of M_1 agonism, so the team decided to revisit the pyrrolo[2,3-*b*]pyridine-based 8¹⁶ and explore an alternate

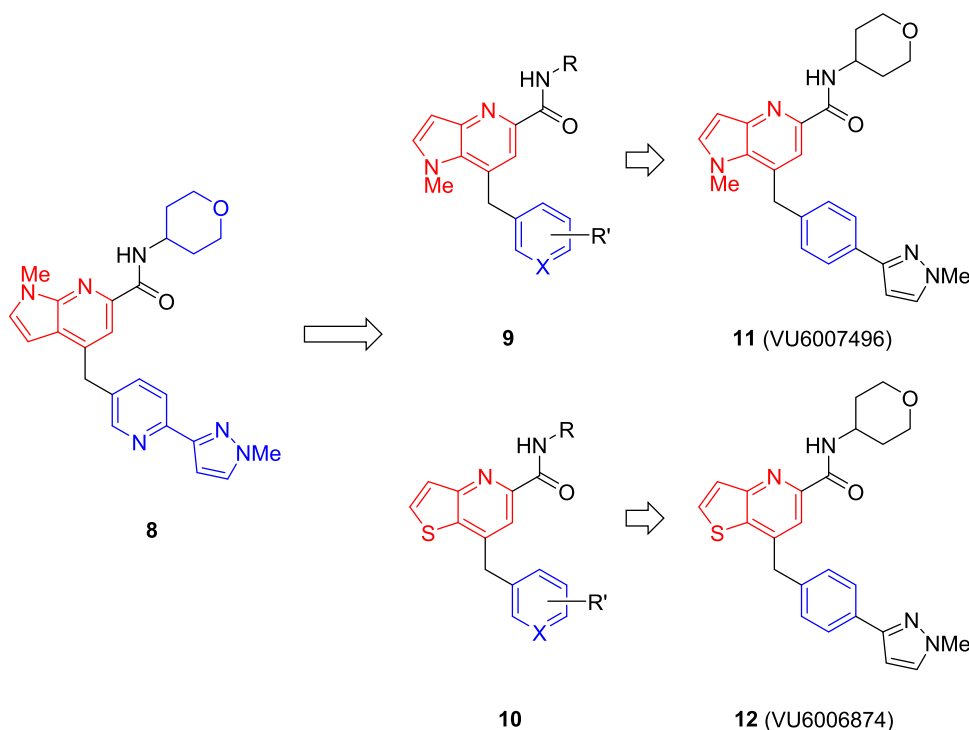


Figure 3. Scaffold-hopping from 8 to regioisomeric cores 9 and 10, which led to the discovery of VU6007496 (11) and VU6006874 (12) that were advanced into further profiling.

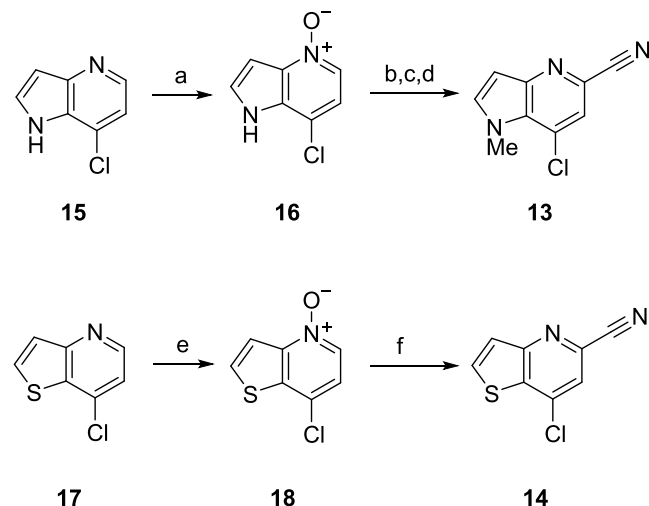
regioisomer, namely a pyrrolo[3,2-*b*]pyridine core 9 as well as an isosteric thieno[3,2-*b*]pyridine core 10 (Figure 3).²¹ Here again, SAR proved to be steep and failed to identify M₁ PAMs with diminished M₁ agonism worthy of further progression toward backup compounds. This exercise led to the discovery of two compounds that advanced into further profiling, VU6007496 (11, a pyrrolo[3,2-*b*]pyridine) and VU6006874 (12, a thieno[3,2-*b*]pyridine), with unexpected results and challenges.

Synthesis. The synthesis of 11 and 12 (Scheme 1) first required the construction of key intermediates, namely a 7-chloro-1-methyl-1*H*-pyrrolo[3,2-*b*]pyridine-5-carbonitrile 13 and a 7-chlorothieryl[3,2-*b*]pyridine-5-carbonitrile 14.²¹ Here, we envisioned that these key intermediates would be prepared from the commercially available chloropyridines 15 and 17 by application of a Reissert-Henze reaction sequence.²² Conversion of 15 to the pyridine *N*-oxide 16 by treatment with *m*-CPBA proceeded in 85% yield. Treatment of 16 with dimethyl sulfate and KCN facilitated the Reissert-Henze reaction followed by *N*-methylation affording the requisite cyanopyridine 13 in 98% over 3 steps. A similar sequence provided the analogous cyanopyridine 14, in albeit lower overall yield (~53% over two steps).²¹

With intermediates 13 and 14 in hand, elaboration into the M₁ PAMs 11 and 12 proved straightforward. Conversion of 13 to the boronate ester 19 proceeded smoothly (Scheme 2), followed by a Suzuki coupling with benzyl chloride 20 to provide 21 in 56% yield for the two steps. Acid-mediated hydrolysis of the nitrile to the carboxylic acid, and a HATU-facilitated coupling with tetrahydro-2*H*-pyran-4-amine delivered 11 in 71% yield for the two step sequence.²¹

Application of a similar reaction sequence with 7-chlorothieryl[3,2-*b*]pyridine-5-carbonitrile 14 provided 12 (Scheme 3). Here, conversion of 14 to the boronate ester 22 proceeded in excellent yield (95%). A Pd(dppf)-

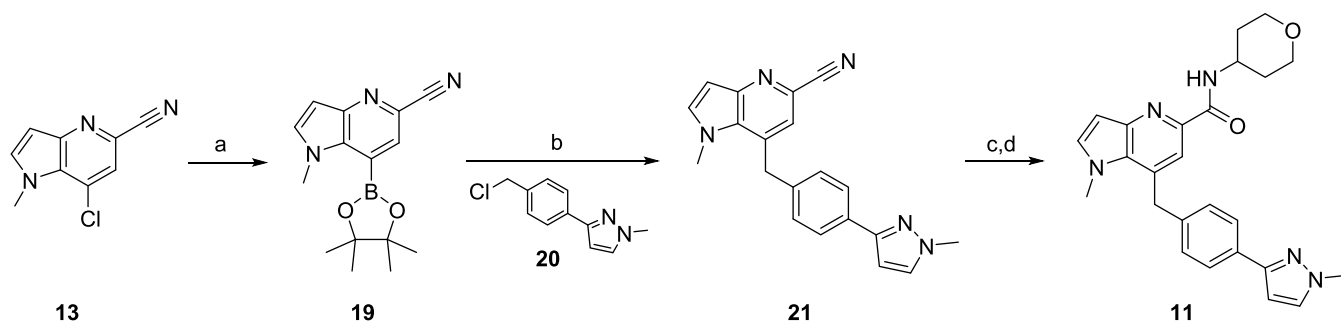
Scheme 1. Synthesis of 7-Chloro-1-methyl-1*H*-pyrrolo[3,2-*b*]pyridine-5-carbonitrile 13 and a 7-Chlorothieryl[3,2-*b*]pyridine-5-carbonitrile 14^a



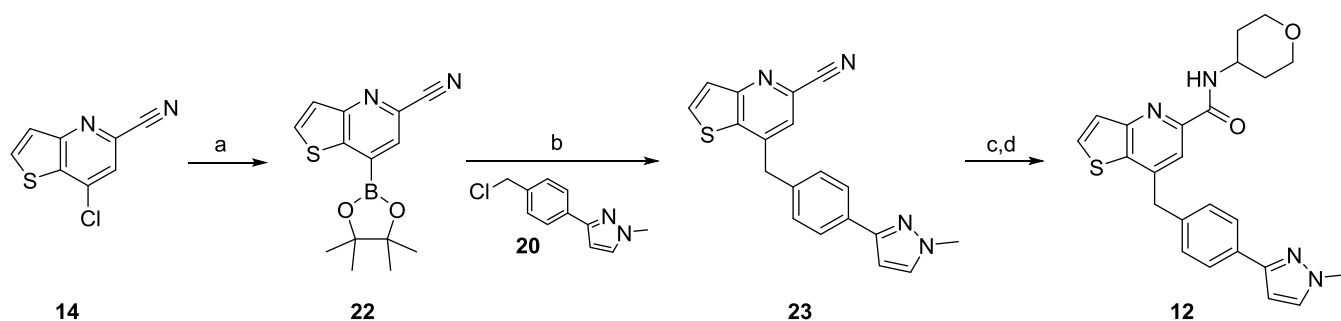
^aReagents and conditions: (a) *m*-CPBA, *n*-BuOAc:heptane (3:5), 0 °C—rt, 83%; (b) (MeO)₂SO₂, *n*-BuOAc, 75 °C, 16 h; (c) KCN, aq. NH₄Cl, 50 °C, 2 h; quantitative yield (2 steps); (d) MeI, NaH, DMF, 0 °C—rt, 98%; (e) *m*-CPBA, DCM, 0 °C—rt, 54%; (f) TMSCN, (CH₃)₂NCOCl, DCM, rt, 16 h, 98%.

Cl₂-catalyzed Suzuki coupling with benzyl chloride 20 gave the elaborated nitrile 23 in 99% isolated yield. Finally, acid-mediated hydrolysis of the nitrile to the acid, and a HATU-facilitated coupling with tetrahydro-2*H*-pyran-4-amine delivered 12 in 61% yield for the two-step sequence.²¹

Molecular Pharmacology and *In Vitro* Drug Metabolism and Pharmacokinetics (DMPK). With 11 and 12 in hand, both compounds were evaluated in a battery of

Scheme 2. Synthesis of VU6007496 (11)^a

^aReagents and conditions: (a) bis(pinacolato)diboron, KOAc, Pd(dppf)Cl₂, 1,4-dioxane, 100 °C, 16 h; (b) benzyl chloride 20, Cs₂CO₃, Pd(dppf)Cl₂, THF/H₂O, 90 °C, 16 h; 56% (2 steps); (c) conc. HCl, reflux, 2 h; (d) tetrahydro-2H-pyran-4-amine, HATU, DIEA, DMF, rt, 20 min, 71% (2 steps).

Scheme 3. Synthesis of VU6006874 (12)^a

^aReagents and conditions: (a) bis(pinacolato)diboron, KOAc, Pd(dppf)Cl₂, 1,4-dioxane, 100 °C, 16 h, 95%; (b) benzyl chloride 20, Cs₂CO₃, Pd(dppf)Cl₂, THF/H₂O, 90 °C, 16 h, 99%; (c) conc. HCl, 100 °C, 3 h; (d) tetrahydro-2H-pyran-4-amine, HATU, DIEA, DMF, rt, 1 h, 61% (2 steps).

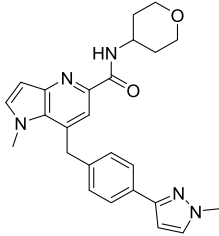
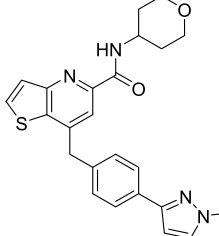
molecular pharmacology and *in vitro* DMPK assays (Table 1) to assess their suitability to advance further down the testing cascade toward putative backup candidates.

On human M₁, 11 was found to be an M₁ PAM (EC₅₀ = 228 nM, 80% ACh max, pEC₅₀ = 6.78 ± 0.11) with minimal M₁ agonism (EC₅₀ > 10 μM, 24% ACh Max), whereas 12 was a more potent M₁ PAM (EC₅₀ = 149 nM, 73% ACh max, pEC₅₀ = 6.88 ± 0.08), but displayed moderate M₁ agonism (EC₅₀ = 3.1 μM, 38% ACh Max).²¹ Both 11 and 12 were potent on rat M₁ with PAM potencies of 94 nM (91% ACh Max) and 63 nM (90% ACh Max), respectively, and both showed moderate rat M₁ agonism. Importantly, both 11 and 12 were inactive on human and rat M₂₋₅ (EC₅₀s > 30 μM). PAMs 11 and 12 displayed moderate predicted hepatic clearance across human, rat and dog; however, both PAMs possessed high predicted hepatic clearance in cyno (≥30 mL/min/kg). Both PAMs showed acceptable plasma and brain homogenate binding profiles, but 12 uniformly showed less fraction unbound. Similarly, both 11 and 12 demonstrated acceptable CYP₄₅₀ profiles against CYP3A4, CYP1A2, CYP2C9 and CYP2D6 (IC₅₀s > 16 μM). In terms of predicted CNS penetration in human, 11 had an MDCK-MDR1 ER ratio of 3.5 with a P_{app} of 12.8, and, based on controls in this assay, was acceptable to move forward, whereas 12 was not a P-gp substrate (ER = 0.8) and had good permeability (P_{app} = 26.8). In a Lead Profiling Screen of 68 GPCRs, ion channels and transporters employing radioligand displacement to assess ancillary pharmacology, 11 had no significant results (<50% displacement at 10 μM), whereas 12 had a single significant hit (melatonin MT1, 70% at 10 μM).²¹ In a 4-strain Ames assay, with and without S9, both

11 and 12 were negative. A GSH trapping study in human liver microsomes to test for reactive intermediates showed similar negative results for the two PAMs. Finally, an electrophysiology panel of cardiac ion channels was clean (<17% inhibition at 10 μM) for both PAMs.²¹ Thus, both PAMs possessed acceptable overall *in vitro* profiles to advance into the tier of the development workflow; however, in the team's opinion, PAM 11 was the leading contender due to higher fraction unbound and less M₁ agonism.

In Vivo Behavior and DMPK. PAMs 11 and 12 were next evaluated in our rat IV plasma: brain level cassette paradigm (0.25 mg/kg compound, 1 mg/kg total dose, 10.1% EtOH:40.4% PEG400:49.5% DMSO) sampled at a set 15 min time point to assess CNS penetration. 11 had a K_p (the partitioning coefficient between plasma and brain) of 0.42 (plasma, 92.2 ng/mL; brain, 39 ng/g) and a K_{p,uu} of 0.36; in contrast, 12 had a K_p of 1.1 (plasma, 105 ng/mL; brain, 120 ng/g) and a K_{p,uu} of 0.7.²⁰ These data were in alignment with the human predicted CNS penetration from the MDCK-MDR1 P-gp *in vitro* assay discussed earlier and supported continued advancement. As mice are the most sensitive species to cholinergic mechanisms,^{11,13,23,24} we placed a high-throughput phenotypic seizure liability assay into the workflow in which potent ago-PAMs, such as 2–5,^{8–15} display robust Racine scale 4/5 behavioral convulsions that develop within minutes of dosing and last for the 3 h duration of the study. Here, a high dose (100 mg/kg intraperitoneal (i.p.)) of either 11 or 12 in mice did not induce seizure liability, akin to 6–9 and VU-319/ACP-319, for the 3-h duration of the study (Figure 4A).²¹ For 11 in particular, the 100 mg/kg i.p. study

Table 1. Pharmacology and *In Vitro* DMPK Profiles of **11** and **12**^a

Structure		
	11	12
VU ID	VU6007496	VU6006874
MW	429.5	432.5
cLogP	4.1	4.4
TPSA	74	69
hM ₁ Agonist EC ₅₀ (nM) [ACh _{max} (%)] (n = 7)	>10,000 [24%]	3,055 [38%]
hM ₁ PAM EC ₅₀ (nM) [ACh _{max} (%)] (n = 7)	228 [80%]	149 [73%]
hM ₂₋₅ EC ₅₀ (nM)	>30,000 (or inactive to be consistent with the abstract figure)	>30,000 (or inactive to be consistent with the abstract figure)
rM ₁ Agonist EC ₅₀ (nM) [ACh _{max} (%)] (n = 4)	7,342 [36%]	4,350 [32%]
rM ₁ PAM EC ₅₀ (nM) [ACh _{max} (%)] (n = 4)	94 [91%]	63 [90%]
rM ₂₋₅ EC ₅₀ (nM)	>30,000 (or inactive to be consistent with the abstract figure)	>30,000 (or inactive to be consistent with the abstract figure)
Predicted CL _{hep} (mL/min/kg) h, r, d, c	12, 38, 14, 31	7.5, 33, 16, 29
f _{u,plasma} (h, r, d, c)	0.016, 0.040, 0.060, 0.026	0.005, 0.015, 0.018, 0.009
f _{u,brain} (r)	0.038	0.011
CYP IC ₅₀ (μM) 1A2, 2C9 2D6, 3A4	>30, 28.5 >30, >30	>30, 16.6 >30, >30
P-gp ER Papp (x 10 ⁻⁶ cm/s)	3.5 12.8	0.8 26.8

^acLogP and TPSA were calculated using ChemDraw Professional 22.2.

afforded total brain exposure of 1.04 μM, and the mouse M₁ PAM EC₅₀ was determined to be 92 nM (66% ACh max). In parallel, we performed electrophysiology studies in mouse native tissue layer V medial prefrontal cortex (mPFC). While ago-PAMs such as 2–5 induce substantial long-term depression that correlates with a lack of robust pro-cognitive efficacy, PAM **11** did not induce significant changes in field excitatory post synaptic potentials (fEPSPs) recorded from layer V and evoked by electrical stimulation in layer II/III at 3 μM concentration (~30x above the functional mouse EC₅₀), and, therefore, maintain activity dependence of PFC function (Figure 4B).²¹ Thus, both compounds cleared the major hurdles of CNS penetration and the liability of M₁ overstimulation.

We next conducted multispecies IV/PO PK in parallel as a potential discerning data set. PAM **11** possessed an attractive PK profile across rat, dog and nonhuman primate (cynom-

logus monkey (cyno)) (Table 2). In rat, **11** showed low-to-moderate clearance (26 mL/min/kg) with a 6.1 h half-life and 66% oral bioavailability. The PK of **11** in dog and cyno was characterized by very low clearance (2.4 and 5.9 mL/min/kg, respectively), long half-life in dog (12.8 h) and a short half-life in cyno (1 h), driven by a low volume (0.39). Oral bioavailability for dog was 35% and cyno was 59%. These data were generated prior to any significant formulation of vehicle screens; thus, we were very pleased with the profile of **11**. PAM **12** was similar in disposition, with moderate clearance (33 mL/min/kg) with a 5.3 h half-life and 100% oral bioavailability in rat. Clearance was low in dog (1.3 mL/min/kg) and cyno (2.3 mL/min/kg), and, once again, a long half-life in dog (36.6 h) and moderate in cyno (4.5 h). However, while oral bioavailability was excellent in rat (100%) and cyno (79%), but it was poor in dog (9%).²¹ With a strong desire to employ dog as the nonrodent safety species, the

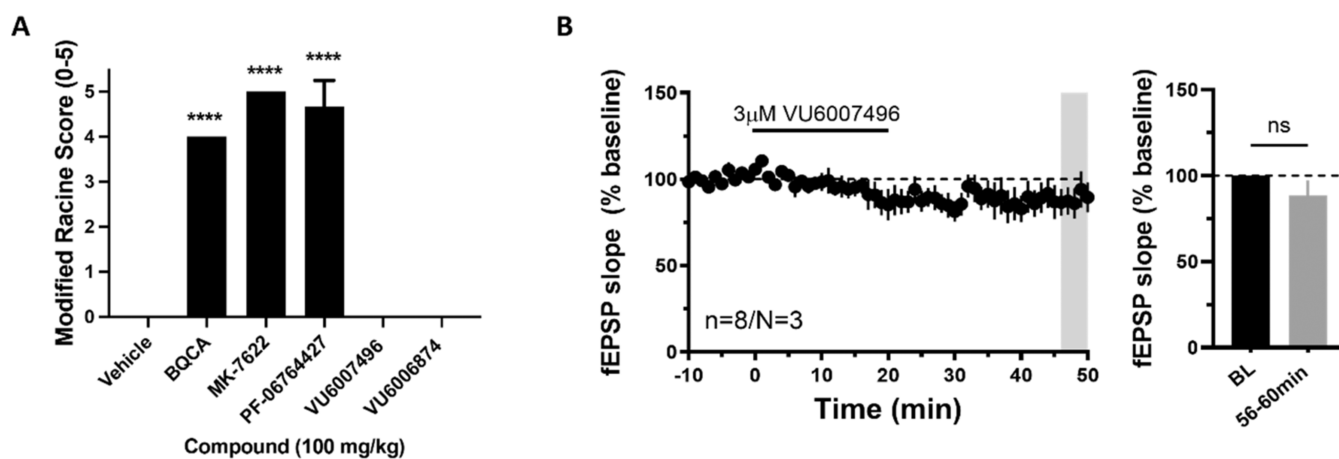


Figure 4. (A) Modified Racine Score test in mice with M_1 PAMs. Pretreatment with M_1 PAMs (100 mg/kg, i.p., 10 mL/kg, 180 min) BQCA (2), MK-7622 (3), PF-06764427 (4), resulted in robust behavioral convulsions at 3 h post administration, while VU6007496 (11) and VU6006874 (12) did not cause any observed adverse effects. $N = 3$ /group of male C57Bl/6 mice. ANOVA $p < 0.0001$; **** $p < 0.0001$ as compared to vehicle control. (B) Time course graph showing that bath application of 3 μ M VU6007496 (11) for 20 min led to no significant change in fEPSP slope. $N = 8$ brain slices from 3 different male C57Bl/6 mice.

Table 2. Pharmacokinetic Parameters of 11

parameter	rat (SD)	dog (beagle or mongrel)	NHP (cyno)
dose (mg/kg) iv/po	1/10	1/5	1/5
CL_p (mL/min/kg)	26	2.4	5.9
V_{ss} (L/kg)	3.2	2.2	0.39
elimination $t_{1/2}$ (h)	6.1	12.8	1.0
F (%) po	66	35	52
K_p	0.42		
$K_{p,uu}$	0.36		

challenge to address the low %F in dog was enough to triage PAM 12 and focus on the advancement of 11 (Table 3).

Table 3. Pharmacokinetic Parameters of 12

parameter	rat Sprague–Dawley (SD)	dog (beagle or mongrel)	NHP (cyno)
dose (mg/kg) iv/po	1/10	1/3	1/3
CL_p (mL/min/kg)	33	1.3	2.3
V_{ss} (L/kg)	8.2	4.0	0.7
elimination $t_{1/2}$ (h)	5.3	36.6	4.5
F (%) po	100	9	79
K_p	1.1		
$K_{p,uu}$	0.7		

Previously, we have shown that potent M_1 ago-PAMs with agonist activity in the PFC showed little efficacy in novel object recognition (NOR); in contrast,^{15,16} M_1 PAMs with no to minimal agonist activity in the PFC displayed robust dose-dependent enhancement of NOR. As illustrated in Figure 5, PAM 11 dose-dependently enhanced recognition memory in rats with a minimum effective dose (MED) of 3 mg/kg p.o., which was in-line with data obtained with previous M_1 PAMs. Interestingly, a 3 mg/kg p.o. rat satellite PK study demonstrated total brain concentration of 990 nM and an unbound brain concentration of 39.8 nM (rat M_1 PAM $EC_{50} = 94$ nM (91% ACh max)). Historically, our PK/PD for M_1 PAMs in NOR has a strong correlation with total brain as opposed to unbound levels, with MEDs typically 0.25 to 0.4 of

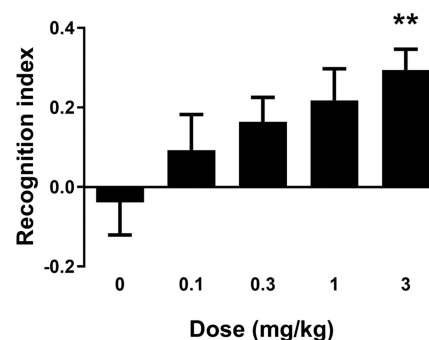


Figure 5. Novel object recognition (NOR) test in rats with VU6007496 (11). PAM 11 dose-dependently enhanced recognition memory in rats. Pretreatment with 0.1, 0.3, 1, and 3 mg/kg VU6007496 (p.o., 0.5% natrosol/0.015% Tween 80 in water, 30 min) prior to exposure to identical objects significantly enhanced recognition memory assessed 24 h later. $N = 15$ –18/group of male Sprague–Dawley rats. ANOVA $p = 0.0283$; ** $p < 0.01$.

the rat EC_{50} .²¹ This may be due to higher endogenous cholinergic tone in healthy animals, and the *in vitro* PAM EC_{50} s being derived from an arbitrarily selected EC_{20} concentration of ACh as a subthreshold value.

In-Depth DMPK Profiling. To advance 11 as a candidate and into IND-enabling studies, we next needed to better understand its CYP profile to minimize drug–drug interactions in the clinic. Here, a substrate depletion approach employing recombinant human cytochrome P450s (rCYPs) indicated that rCYP2J2 and rCYP3A4 are responsible for 2.4 and 97.6% of the hepatic CYP-mediated clearance of PAM 11, respectively. We were pleased to see the contribution of another CYP beyond 3A4 for the metabolism of 11.²¹ In parallel, we investigated the ability of PAM 11 to induce the expression of CYP₄₅₀s (measuring mRNA) in cryopreserved human hepatocytes from three separate donors. Weak induction liability was noted for CYP1A2 (~3-fold) and CYP2B6 (~8-fold), while more concerning induction liability was reported for CYP3A4 (~21-fold), and would require subsequent evaluation using the assessment of protein expression instead of mRNA.²¹

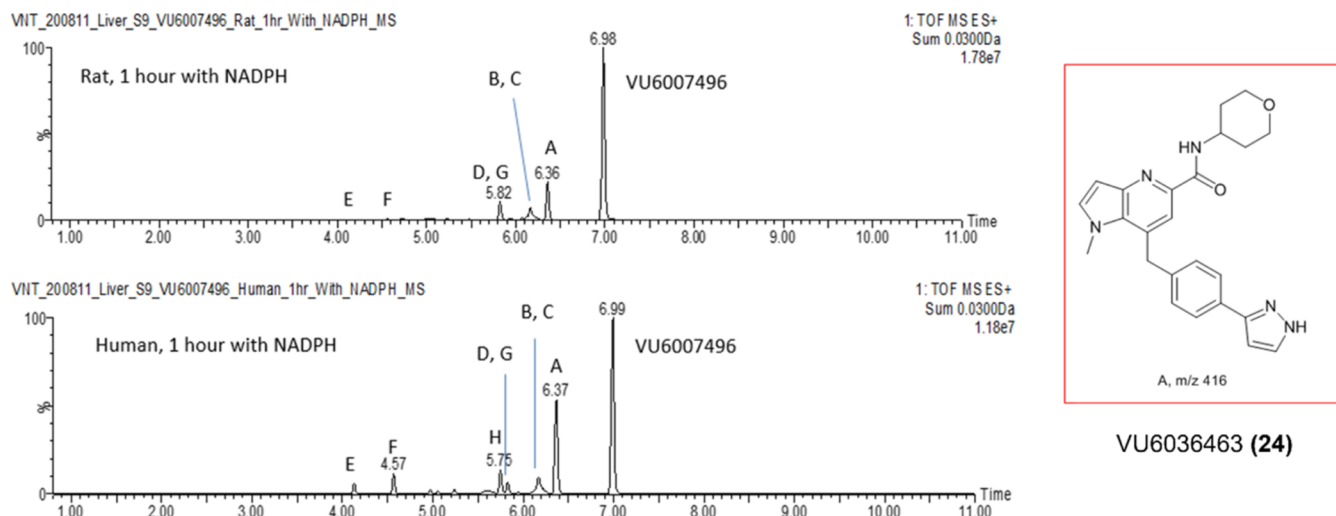
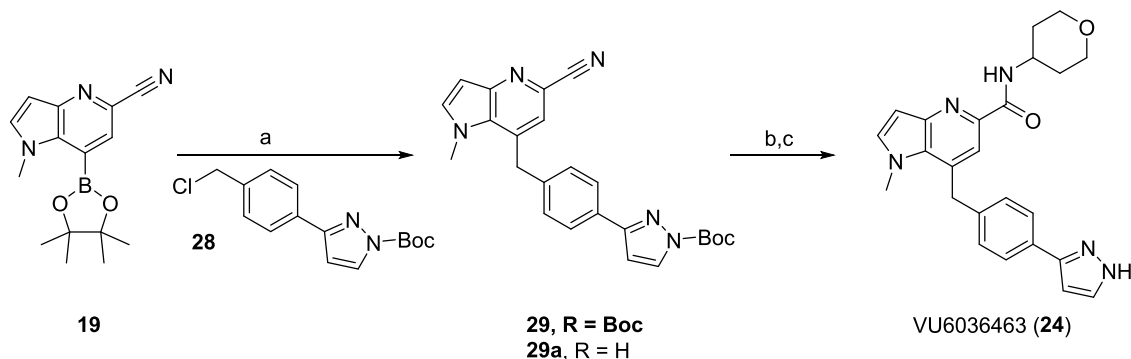


Figure 6. Metabolism of VU6007496 (**11**) in rat and human liver S9, with the major metabolite, VU6036463 (**24**), an *N*-demethylation product, exemplified.

Scheme 4. Synthesis of Metabolite VU6036463 (**24**)^a



^aReagents and conditions: (a) benzyl chloride **28**, Cs₂CO₃, Pd(dppf)Cl₂, THF/H₂O, 90 °C, 16 h; 58%; (b) conc. HCl, reflux, 2 h; (c) tetrahydro-2*H*-pyran-4-amine, HATU, DIEA, DMF, rt, 20 min, 81% (2 steps).

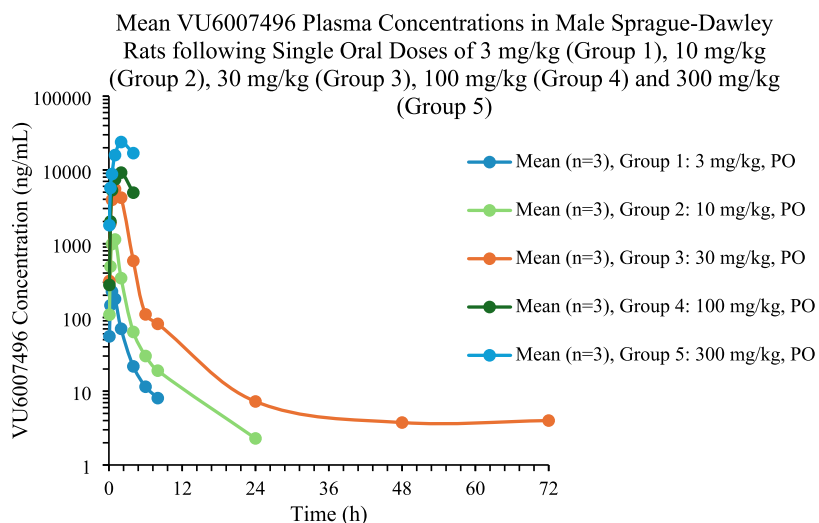


Figure 7. Rat dose escalation study with VU6007496 (**11**).

In parallel to these CYP studies, we performed metabolite identification (MET ID) studies in rat and human S9 liver microsomes (Figure 6) and observed comparable coverage of metabolites across human and rat. The PAM **11** proved to be

reasonably stable, with the extent of metabolism being 36.8% in rat and 58.1% in human (based on MS peak areas). Eight oxidative metabolites were identified, with the major metabolite in both rat and human being Metabolite A

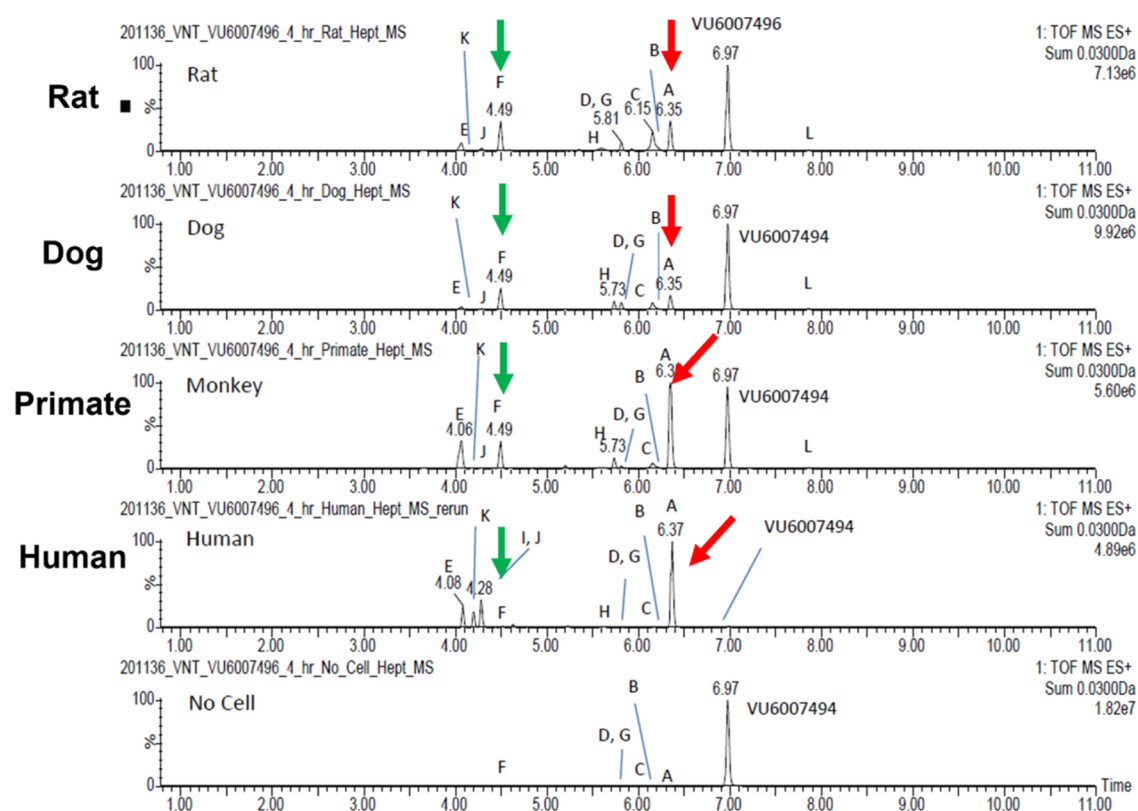


Figure 8. Metabolism of VU6007496 (**11**) in rat, dog, primate and human hepatocytes, with the major metabolite, VU6036463 (**24**), an *N*-demethylation product. Unexpectedly, no parent PAM **11** remained in human after the 4 h incubation.

(VU6036463, **24**), the result of oxidative *N*-demethylation of the southern pyrazole (Scheme 4). The majority of other oxidative metabolism occurred on the tetrahydropyran moiety and included ring opening, but there was no amide hydrolysis observed.²¹

While awaiting more definitive MET ID studies in multispecies hepatocytes, we elected to perform a rat dose escalation study to assess exposures in a standard, tox-friendly oral vehicle (30% captisol) to lay the foundation for dose range finding/maximum tolerated dose (DRF/MTD) studies. Male Sprague–Dawley rats were dosed with VU6007496 (**11**) at doses of 3, 10, 30, 100, and 300 mg/kg p.o. in 30% captisol. At all doses, PAM **11** was rapidly absorbed with tight T_{max} values under 2 h (Figure 7). Linear dose escalation was noted from 3 to 30 mg/kg. However, severe adverse cholinergic events were noted after 4.5 h in the 100 and 300 mg/kg dose groups which was not expected due to the clean mouse phenotypic assay and our long history with other M_1 PAMs.²⁰ Recall, exposures in rat at the NOR MED were 990 nM total and 39.8 nM unbound brain concentrations, respectively. At C_{max} the 100 mg/kg dose achieved 9.1 μ M total and 298 nM unbound brain concentrations (\sim 9-fold over the NOR MED exposure), while the 300 mg/kg dose afforded 17.2 μ M total and 569 nM unbound brain concentrations (\sim 17-fold over the NOR MED exposure).²¹ There was a clear, yet unanticipated disconnect.

More concerning were the results generated *via* outsourced multispecies hepatocyte MET ID, which were drastically different than the liver S9 MET ID. The extent of metabolism for VU6007496 with rat, dog, monkey and human hepatocytes was 64.7, 51.5, 63.9 and 99.5%, respectively (Figure 8). Twelve metabolites were observed in the 4-h hepatocytes samples, and as opposed to the S9 study, there was no parent **11** remaining

in human hepatocytes. In human hepatocytes, PAM **11** was metabolized primarily to Metabolite A (**24**), the result of oxidative *N*-demethylation of the southern pyrazole. The other minor metabolites were oxidation on the tetrahydropyran moiety and included ring opening (Metabolite F, **25**).²¹ With these data, PAM **11** was no longer a backup candidate, but the disconnects and paradigm changing cholinergic toxicity profile warranted further investigation to inform the next backup campaign.

We typically would not examine mouse hepatocyte MET ID, as mouse was not a safety species for the IND-enabling toxicology package, but with the unusual metabolism profile for human, and the lack of predictive cholinergic tox in the mouse phenotypic assay, we felt this was worthy of exploration. As shown in Figure 9, PAM **11** rapidly undergoes extensive metabolism (95.4%) on the tetrahydropyran moiety and almost complete ring opening to the hydroxy acid Metabolite F (**25**).²¹ Clearly, based on the hepatocyte data, there is a tremendous difference in the concentration of parent **11** and metabolite composition, which sheds light on the mouse-rat disconnect for observed cholinergic toxicity in rat *versus* the more cholinergic sensitive mouse.

The team was still puzzled by the severe cholinergic adverse events observed in rats at the 100 and 300 mg/kg arms of the dose escalation study, as this was not consistent with the past 20 years of M_1 PAM research. Could the *N*-demethylated metabolite A (**24**) be responsible? Due to the disconnect between liver S9 and hepatocytes, we felt it was prudent to examine *in vivo* rat MET ID at doses of 100 and 300 mg/kg to ensure **24** is produced upon *in vivo* oral dosing after 5–30 min and 160–240 min, and to determine if any other putative metabolites are generated at detectable levels (Figure 10).

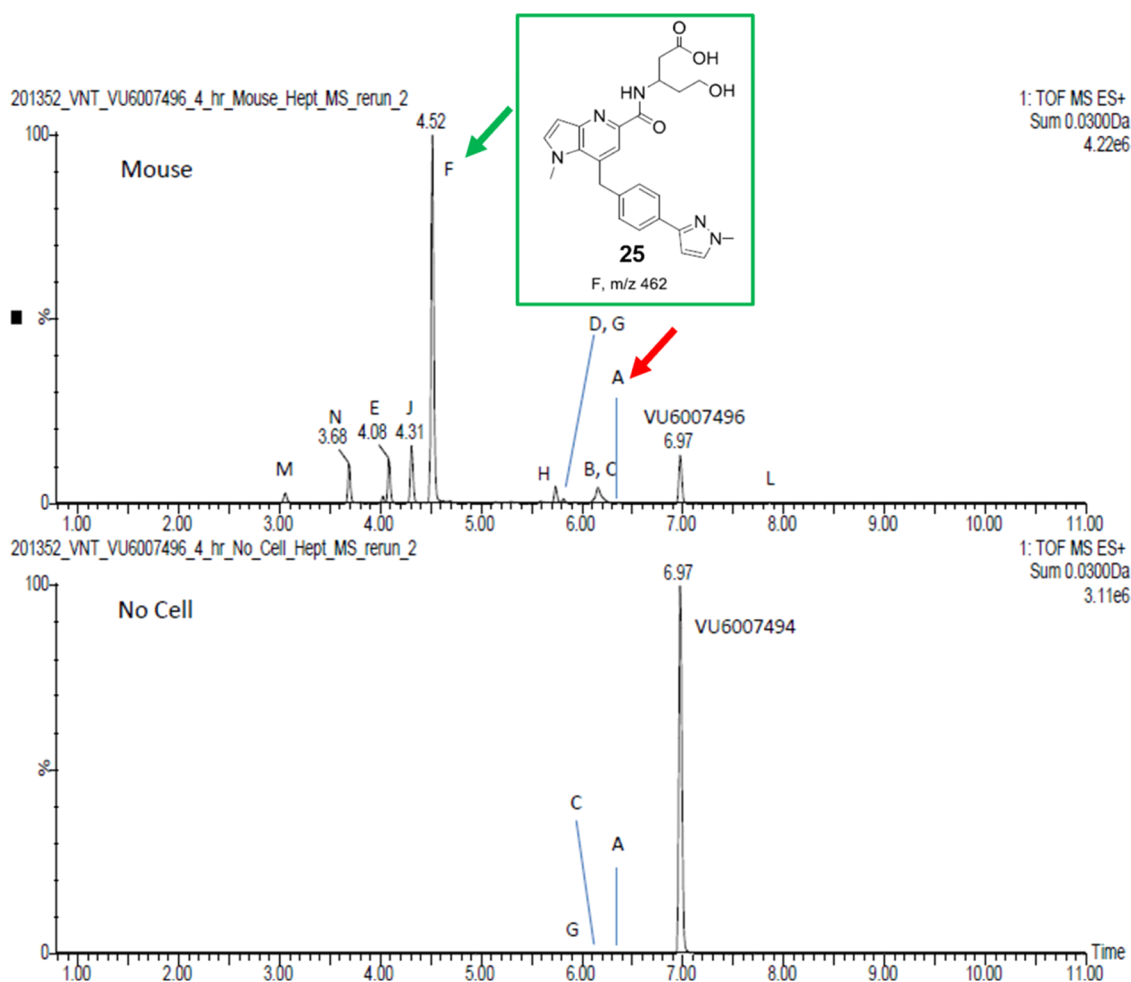


Figure 9. Extensive metabolism (95.4%) of VU6007496 (**11**) in mouse hepatocytes, with metabolite F (**25**) produced in high abundance.

Across both doses and time points, 73–81% of the parent **11** remained. Metabolite **24** was produced *in vivo* at 2.2 to 5.6% relative abundance and lower than from *in vitro* incubations, along with two oxidative metabolites, a dioxygenated species M461 (**26**) and a mono-oxygenated species M445 (**27**) on the tetrahydropyran moiety. These were produced in higher relative abundance than **24**, representing 7.7 to 13.8% (**26**) and 8.3 to 11.1% (**27**), respectively.²¹ A species such as **27** would resemble the hydroxy pyranyl congeners known to be potent ago-PAMs and prone to severe cholinergic side effects, and the potential for **24** to elicit similar cholinergic toxicity was unknown. However, it was clear from these data that PAM **11** rapidly generated stable metabolites with strong potential to be “active” metabolites.

Synthesis and Characterization of Metabolites. Due to the prevalence of metabolite A (VU6036463, **24**) in both *in vitro* preparations and *in vivo*, we first synthesized and characterized **24**. Utilizing intermediate **19** (Scheme 3), a Suzuki coupling with benzyl chloride **28** afforded a mixture of *N*-Boc protected analog **29** and *N*-H analog **29a** in moderate isolated yield. Hydrolysis of the nitriles to the carboxylic acid, followed by a HATU-mediated coupling with tetrahydro-2*H*-pyran-4-amine delivered **24** in 81% yield over the two steps.²¹ In our kinetic assays, **24** was an “active” metabolite, with the profile of an M₁ ago-PAM. Metabolite **24** was a potent M₁ PAM on both rat (EC₅₀ = 56 nM, 89% ACh max) and human (EC₅₀ = 144 nM, 73% ACh max); in fact, more potent than the

parent **11**. PAM **24** also displayed M₁ agonism at both the rat (EC₅₀ = 3.1 μM, 48% ACh Max) and human receptors (EC₅₀ = 2.1 μM, 36% ACh Max). As with the parent **11**, metabolite **24** was inactive on rat and human M₂₋₅. In our tier 1 *in vitro* DMPK panel, **24** displayed an acceptable profile with moderate predicted hepatic clearance (hCL_{hep} = 12.8 mL/min/kg and rCL_{hep} = 44 mL/min/kg), good unbound fraction in human (*f*_u = 0.047), rat (*f*_u = 0.134) and rat brain homogenate binding (*f*_u = 0.025), and an acceptable CYP profile (>30 μM @ 1A2, 2C9, 2D6 and 5.7 μM @ 3A4). To ascertain if **24** could be the source of the adverse cholinergic events in rats, we dosed **11** and **24**, in parallel, at a dose of 100 mg/kg i.p. in 30% captisol and prepared plasma and brain samples at a 3-h time point to determine brain exposure of the M₁ ago-PAM **24**. In this study, **11** achieved a total plasma concentration of 3.6 μM and a total brain concentration of 0.93 μM (*K*_p = 0.26). In contrast, and again—unexpectedly—the metabolite **24** displayed lower exposure in plasma (1.2 μM) and very low (0.08 μM) brain exposure (*K*_p = 0.07).²¹ These data suggest that the adverse events in rats was unlikely due to CNS activity of the “active” metabolite **24**. To further confirm this *in vivo* finding, **24** was found to be a P-gp substrate (MDR1-MDCK ER = 31.9, *P*_{app} = 2.0 × 10⁻⁶ cm/s) rendering **24** a nonparticipant in the observed toxicity of **11**. At the same time, we explored an *N*-CD₃ congener of **11** to determine if the kinetic isotope effect would engender metabolic stability to the alkylated pyrazole and avoid the

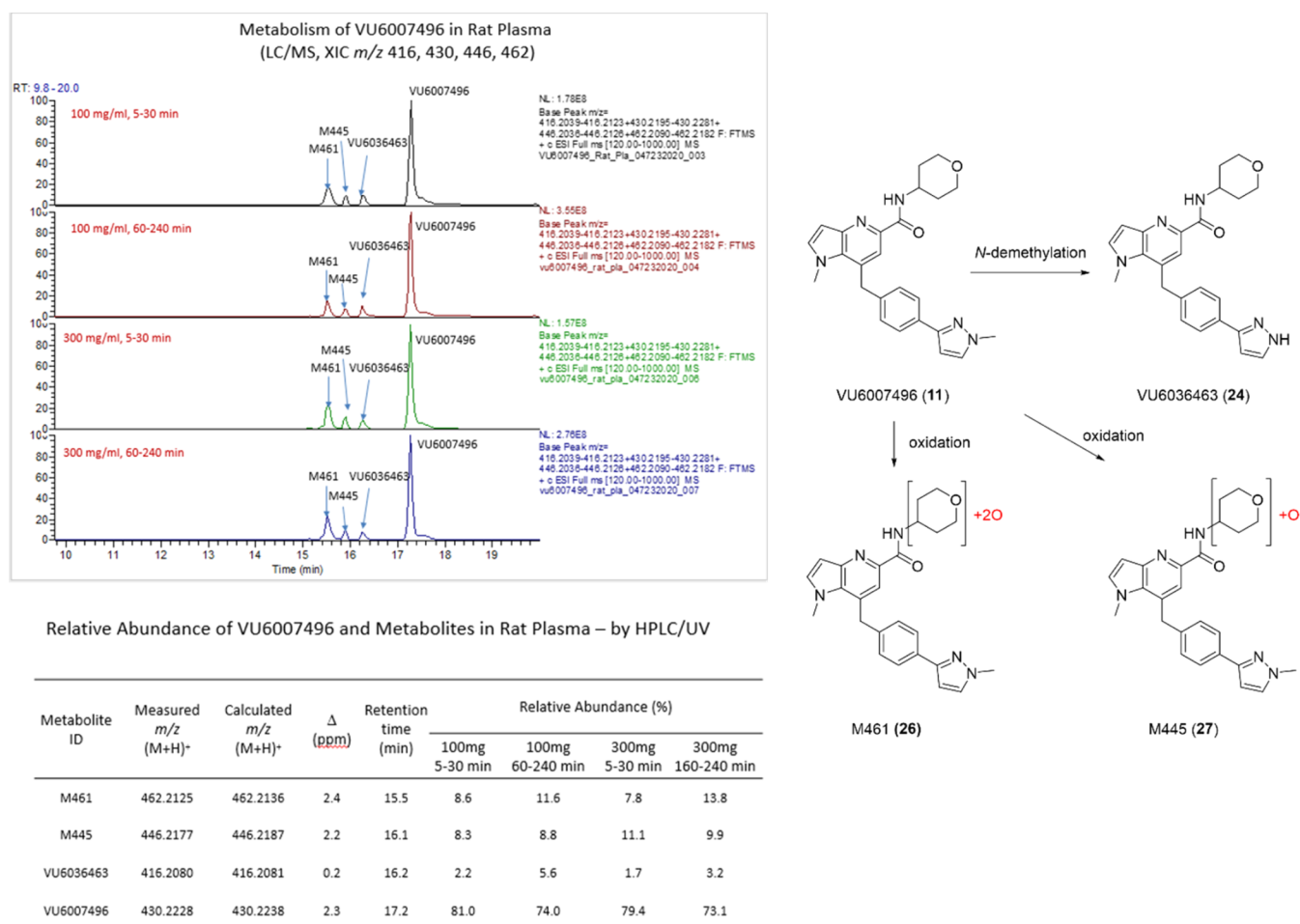


Figure 10. *In vivo* MET ID and metabolic pathways of VU6007496 (**11**) in mouse rat plasma at 100 mg/kg and 300 mg/kg p.o. at 5–30 min and 160–240 min at each dose. Three metabolites are produced *in vivo*: the *N*-demethylated **24**, and two oxidative metabolites, a dioxxygenated species M461 (**26**) and a mono-oxygenated species M445 (**27**) on the tetrahydropyranly moiety.

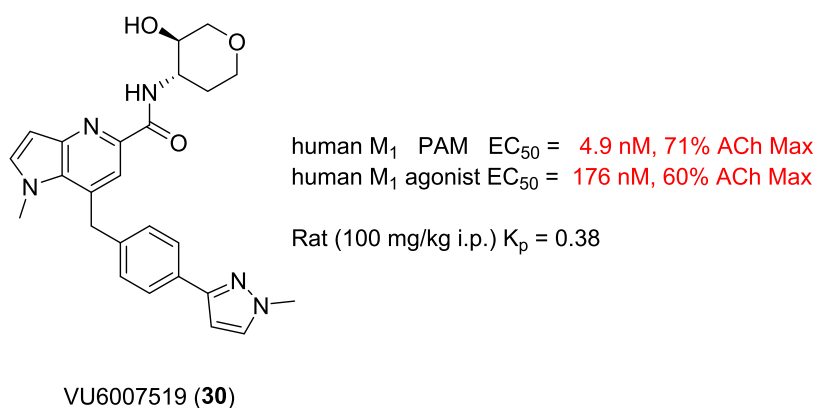


Figure 11. Structure and human M_1 pharmacology of **30**, an extremely potent M_1 ago-PAM with CNS penetration in rat.

production of **24**, but the metabolism proved to be identical to the *N*-CH₃.

Based on the known cholinergic adverse events with hydroxy pyranlyl amides such as **2–5**,^{8–12} and the rat *in vivo* MET ID suggesting, by mass, that M445 (**27**) was a similar species, we prepared analog **30** (VU6007519) following Scheme 2. As shown in Figure 11, this putative metabolite was an extremely potent human M_1 ago-PAM (PAM EC_{50} = 4.9 nM, 71% ACh Max; agonist EC_{50} = 176 nM, 60%), and this profile would

likely give rise to the cholinergic adverse events seen in rats at doses over 100 mg/kg. Importantly, **30** was also brain penetrant in rat at 100 mg/kg i.p. (K_p = 0.38) and comparable to **11** (K_p = 0.26). To provide additional evidence that this “active” metabolite was responsible for the overactivation of M_1 and the observed toxicity, coinjection of **30** with the rat *in vivo* MET ID proved that **30** was not in fact the metabolite 445 (**27**) despite identical masses.²¹ Thus, **27** was possibly another stereo- or regio-isomer of **30**, but quite likely a potent M_1 ago-

PAM. While a valuable and interesting line of investigation, the project team had to refocus on ligands with the potential to advance as backups to our clinical asset, VU319/ACP-319.

CONCLUSIONS

In summary, a lead optimization campaign to identify a suitable backup for the clinical compound, VU319/ACP-319, focused on scaffold-hopping from the pyrrolo[2,3-*b*]pyridine-based M₁ PAM, VU6007477, to isomeric pyrrolo[3,2-*b*]pyridine and thieno[3,2-*b*]pyridine congeners. From this effort, VU6007496, a pyrrolo[3,2-*b*]pyridine, advanced into late stage profiling, only to be plagued with unanticipated, species-specific metabolism, *in vitro/in vivo* disconnects and “active” and potentially toxic metabolites. For this program, *in vitro* liver S9, hepatocyte and *in vivo* MET ID were critical to identify putative “active” metabolites. The unexpected and species-specific mouse metabolism thwarted our phenotypic cholinergic seizure liability *in vivo* screen as a stage gate, and thus prevented further development of VU6007496 as a backup clinical candidate. However, VU6007496 proved to be a highly selective and CNS penetrant M₁ PAM (with minimal agonism), with excellent multispecies IV/PO PK, CNS penetration, no impact on long-term depression (or cholinergic toxicity) and robust efficacy in novel object recognition (MED = 3 mg/kg p.o.). Cholinergic toxicity was not observed in rats at 30 mg/kg p.o., providing a 10-fold window from the MED, and suggesting that VU6007496 can serve as another valuable *in vivo* rat tool compound, but not mouse, to study selective M₁ activation *in vivo*.

ASSOCIATED CONTENT

Supporting Information

The Supporting Information is available free of charge at <https://pubs.acs.org/doi/10.1021/acscemneuro.4c00508>.

Additional experimental details; methods for the synthesis and characterization of all compounds; *in vitro* and *in vivo* DMPK protocols; eurofins lead profiling screen data; synthesis of VU6006874 (12) (PDF)

AUTHOR INFORMATION

Corresponding Author

Craig W. Lindsley – Warren Center for Neuroscience Drug Discovery, Vanderbilt University, Nashville, Tennessee 37232, United States; Department of Pharmacology, Vanderbilt University School of Medicine, Nashville, Tennessee 37232, United States; Department of Chemistry, Vanderbilt University, Nashville, Tennessee 37232, United States; Vanderbilt Kennedy Center, Vanderbilt University Medical Center, Nashville, Tennessee 37232, United States; orcid.org/0000-0003-0168-1445; Phone: 615-322-8700; Email: craig.lindsley@vanderbilt.edu

Authors

Julie L. Engers – Warren Center for Neuroscience Drug Discovery, Vanderbilt University, Nashville, Tennessee 37232, United States; Department of Pharmacology, Vanderbilt University School of Medicine, Nashville, Tennessee 37232, United States; orcid.org/0009-0004-3654-5464
Katrina A. Bollinger – Warren Center for Neuroscience Drug Discovery, Vanderbilt University, Nashville, Tennessee 37232, United States; Department of Pharmacology, Vanderbilt

University School of Medicine, Nashville, Tennessee 37232, United States

Rory A. Capstick – Warren Center for Neuroscience Drug Discovery, Vanderbilt University, Nashville, Tennessee 37232, United States; Department of Pharmacology, Vanderbilt University School of Medicine, Nashville, Tennessee 37232, United States

Madeline F. Long – Warren Center for Neuroscience Drug Discovery, Vanderbilt University, Nashville, Tennessee 37232, United States; Department of Pharmacology, Vanderbilt University School of Medicine, Nashville, Tennessee 37232, United States; orcid.org/0000-0002-8933-3439

Aaron M. Bender – Warren Center for Neuroscience Drug Discovery, Vanderbilt University, Nashville, Tennessee 37232, United States; Department of Pharmacology, Vanderbilt University School of Medicine, Nashville, Tennessee 37232, United States

Jonathan W. Dickerson – Warren Center for Neuroscience Drug Discovery, Vanderbilt University, Nashville, Tennessee 37232, United States; Department of Pharmacology, Vanderbilt University School of Medicine, Nashville, Tennessee 37232, United States

Weimin Peng – Warren Center for Neuroscience Drug Discovery, Vanderbilt University, Nashville, Tennessee 37232, United States; Department of Pharmacology, Vanderbilt University School of Medicine, Nashville, Tennessee 37232, United States

Christopher C. Presley – Warren Center for Neuroscience Drug Discovery, Vanderbilt University, Nashville, Tennessee 37232, United States; Department of Pharmacology, Vanderbilt University School of Medicine, Nashville, Tennessee 37232, United States

Hyekyung P. Cho – Warren Center for Neuroscience Drug Discovery, Vanderbilt University, Nashville, Tennessee 37232, United States; Department of Pharmacology, Vanderbilt University School of Medicine, Nashville, Tennessee 37232, United States

Alice L. Rodriguez – Warren Center for Neuroscience Drug Discovery, Vanderbilt University, Nashville, Tennessee 37232, United States; Department of Pharmacology, Vanderbilt University School of Medicine, Nashville, Tennessee 37232, United States; orcid.org/0000-0002-5244-5103

Colleen M. Niswender – Warren Center for Neuroscience Drug Discovery, Vanderbilt University, Nashville, Tennessee 37232, United States; Department of Pharmacology, Vanderbilt University School of Medicine, Nashville, Tennessee 37232, United States; Vanderbilt Kennedy Center, Vanderbilt University Medical Center, Nashville, Tennessee 37232, United States; Vanderbilt Brain Institute and Vanderbilt Institute of Chemical Biology, Vanderbilt University, Nashville, Tennessee 37232, United States

Sean P. Moran – Warren Center for Neuroscience Drug Discovery, Vanderbilt University, Nashville, Tennessee 37232, United States; Department of Pharmacology, Vanderbilt University School of Medicine, Nashville, Tennessee 37232, United States; orcid.org/0000-0001-7672-242X

Zixiu Xiang – Warren Center for Neuroscience Drug Discovery, Vanderbilt University, Nashville, Tennessee 37232, United States; Department of Pharmacology, Vanderbilt University School of Medicine, Nashville, Tennessee 37232, United States

Anna L. Blobaum – Warren Center for Neuroscience Drug Discovery, Vanderbilt University, Nashville, Tennessee 37232,

United States; Department of Pharmacology, Vanderbilt University School of Medicine, Nashville, Tennessee 37232, United States

Olivier Boutaud – Warren Center for Neuroscience Drug Discovery, Vanderbilt University, Nashville, Tennessee 37232, United States; Department of Pharmacology, Vanderbilt University School of Medicine, Nashville, Tennessee 37232, United States

Jerri M. Rook – Warren Center for Neuroscience Drug Discovery, Vanderbilt University, Nashville, Tennessee 37232, United States; Department of Pharmacology, Vanderbilt University School of Medicine, Nashville, Tennessee 37232, United States

Darren W. Engers – Warren Center for Neuroscience Drug Discovery, Vanderbilt University, Nashville, Tennessee 37232, United States; Department of Pharmacology, Vanderbilt University School of Medicine, Nashville, Tennessee 37232, United States

P. Jeffrey Conn – Warren Center for Neuroscience Drug Discovery, Vanderbilt University, Nashville, Tennessee 37232, United States; Department of Pharmacology, Vanderbilt University School of Medicine, Nashville, Tennessee 37232, United States; Vanderbilt Kennedy Center, Vanderbilt University Medical Center, Nashville, Tennessee 37232, United States

Complete contact information is available at:

<https://pubs.acs.org/10.1021/acschemneuro.4c00508>

Author Contributions

C.W.L., D.W.E., P.J.C., C.M.N., J.K.R., A.L.B., O.B. A.L.R. and H.P.C. oversaw the medicinal chemistry, target selection and interpreted biological/DMPK data. C.W.L. wrote the manuscript. J.L.E., K.A.B., R.A.C., M.F.L., A.M.B., D.W.E. performed chemical synthesis. C.C.P. performed and analyzed HRMS reports. H.P.C., A.L.R. and C.M.N. performed and analyzed *in vitro* pharmacology assays. S.P.M. and Z.X. and S.P.M. performed slice electrophysiology studies. J.W.D., W.P. and J.M.R. performed *in vivo* behavior pharmacology assays and *in vivo* DMPK. A.L.B. and O.B. performed *in vitro* and *in vivo* DMPK studies. All authors have given approval to the final version of the manuscript.

Funding

Studies were supported by NIH (NIMH, MH082867, MH073676 and MH108498) and Acadia Pharmaceuticals (UNIV61505).

Notes

The authors declare the following competing financial interest(s): We hold U.S. patents on M1 PAMs (the chemical series in this article are no longer under development) and are working with Acadia Pharmaceuticals on new, distinct chemical matter.

ACKNOWLEDGMENTS

The authors thank William K. Warren, Jr., and the William K. Warren Foundation for support of our programs and endowing both the Warren Center for Neuroscience Drug Discovery and the William K. Warren, Jr., Chair in Medicine (C.W.L.).

ABBREVIATIONS

PAM, positive allosteric modulator; PBL, plasma/brain level; DMPK, drug metabolism and pharmacokinetics; AE, adverse

event; M₁, muscarinic acetylcholine receptor subtype 1; MED, minimum effective dose; NOR, novel object recognition

REFERENCES

- (1) Bodick, N. C.; Offen, W. W.; Levey, A. I.; Cutler, N. R.; Gauthier, S. G.; Satlin, A.; Shannon, H. E.; Tollefson, G. D.; Rasmussen, K.; Bymaster, F. P.; Hurley, D. J.; et al. Effects of xanomeline, a selective muscarinic receptor agonist, on cognitive function and behavioral symptoms in Alzheimer disease. *Arch. Neurol.* **1997**, *54* (4), 465–473.
- (2) Shekhar, A.; Potter, W. Z.; Lightfoot, J.; Lienemann, D.; Dube, S.; Mallinckrodt, C.; Bymaster, F. P.; McKinzie, D. L.; Felder, C. C. Selective muscarinic receptor agonist xanomeline as a novel treatment approach for schizophrenia. *Am. J. Psychiatry.* **2008**, *165*, 1033–1039.
- (3) Brannan, S. K.; Sawchak, S.; Miller, A. C.; Lieberman, J. A.; Paul, S. M.; Brier, A. Muscarinic Cholinergic Receptor Agonist and Peripheral Antagonist for Schizophrenia. *N. Engl. J. Med.* **2021**, *384* (8), 717–726.
- (4) Melancon, B. J.; Tarr, J. C.; Panarese, J. D.; Wood, M. R.; Lindsley, C. W. Allosteric modulation of the M1 muscarinic acetylcholine receptor: improving cognition and a potential treatment for schizophrenia and Alzheimer's disease. *Drug Discovery Today* **2013**, *18* (23–24), 1185–1199.
- (5) Bridges, T. M.; LeBois, E. P.; Hopkins, C. R.; Wood, M. R.; Jones, J. K.; Conn, P. J.; Lindsley, C. W. Antipsychotic potential of muscarinic allosteric modulation. *Drug News Perspect.* **2010**, *23*, 229–240.
- (6) Nguyen, H. T. M.; van der Westhuizen, E. T.; Langmead, C. J.; Tobin, A. B.; Sexton, P. M.; Christopoulos, A.; Valant, C. Opportunities and challenges for the development of M1 muscarinic receptor positive allosteric modulators in the treatment for neurocognitive deficits. *Br. J. Pharmacol.* **2024**, *181* (14), 2114–2142.
- (7) Dwomoh, L.; Rossi, M.; Scarpa, M.; Khajehali, E.; Molloy, C.; Herzyk, P.; Bottrill, A. R.; Sexton, P. M.; Christopoulos, A.; Conn, P. J.; Lindsley, C. W.; Bradley, S. J.; Tobin, A. B. M₁ muscarinic receptor activation reduces pathology and slows the progression of prion-mediated neurodegenerative diseases. *Sci. Signaling* **2022**, *15*, No. eabm3720.
- (8) Ma, L.; Seager, M.; Wittman, M.; Bickel, N.; Burno, M.; Jones, K.; Graufelds, V. K.; Xu, G.; Pearson, M.; McCampbell, A.; Gaspar, R.; Shughrue, P.; Danzinger, A.; Regan, C.; Garson, S.; Doran, S.; Kreatsoulas, C.; Veng, L.; Lindsley, C. W.; Shipe, W.; Kuduk, S.; Jacobson, M.; Sur, C.; Kinney, G.; Seabrook, G. R.; Ray, W. J.; et al. Selective activation of the M1 muscarinic acetylcholine receptor achieved by allosteric potentiation. *Proc. Natl. Acad. Sci. U.S.A.* **2009**, *106*, 15950–15955.
- (9) Shirey, J. K.; Brady, A. E.; Jones, P. J.; Davis, A. A.; Bridges, T. M.; Jadhav, S. B.; Menon, U.; Christain, E. P.; Doherty, J. J.; Quirk, M. C.; Snyder, D. H.; Levey, A. I.; Watson, M. L.; Nicolle, M. M.; Lindsley, C. W.; Conn, P. J. A selective allosteric potentiator of the M₁ muscarinic acetylcholine receptor increases activity of medial prefrontal cortical neurons and can restore impairments of reversal learning. *J. Neurosci.* **2009**, *29*, 14271–14286.
- (10) Beshore, D. C.; Di Marco, C. N.; Chang, R. K.; Greshock, T. J.; Ma, L.; Wittman, M.; Seager, M. A.; Koeplinger, K. A.; Thompson, C. D.; Fuerst, J.; Hartman, G. D.; Bilodeau, M. T.; Ray, W. J.; Kuduk, S. D. MK-7622: A first-in-class M1 positive allosteric modulator development candidate. *ACS Med. Chem. Lett.* **2018**, *9*, 652–656.
- (11) Moran, S. P.; Dickerson, J. W.; Plumley, H. C.; Xiang, Z.; Maksymetz, J.; Remke, D. H.; Doyle, C. A.; Niswender, C. M.; Engers, D. W.; Lindsley, C. W.; Rook, J. M.; Conn, P. J.; et al. M₁ positive lacking agonist activity provide the optimal profile for enhancing cognition. *Neuropsychopharmacology* **2018**, *43*, 1763–1771.
- (12) Davoren, J. E.; Garnsey, M.; Pettersen, B.; Brodeney, M. A.; Edgerton, J. R.; Fortin, J.-P.; Grimwood, S.; Harris, A. R.; Jenkison, S.; Kenakin, T.; Lazzaro, J. T.; Lee, C.-W.; Lotarski, S. M.; Nottebaum, L.; O'Neil, S. V.; Popiolek, M.; Ramsey, S.; Steyn, S. J.; Thorn, C. A.; Zhang, L.; Webb, D. Design and synthesis of γ - and δ -lactam M₁ positive allosteric modulators (PAMs): convulsion and cholinergic

toxicity of M₁-selective PAM with weak agonist activity. *J. Med. Chem.* **2017**, *60*, 6649–6663.

(13) Moran, S. P.; Cho, H. P.; Maksymetz, J.; Remke, D.; Hanson, R.; Niswender, C. M.; Lindsley, C. W.; Rook, J. M.; Conn, P. J. PF-06827443 displays robust allosteric agonist and positive allosteric modulator activity in high receptor reserve and native systems. *ACS Chem. Neurosci.* **2018**, *9*, 1572–1581.

(14) Rook, J. M.; Abe, M.; Cho, H. P.; Nance, K. D.; Luscombe, V. B.; Adams, J. J.; Dickerson, J. W.; Remke, D. H.; Garcia-Barrantes, P. M.; Engers, D. W.; Engers, J. L.; Chang, S.; Foster, J. J.; Blobaum, A. L.; Niswender, C. M.; Jones, C. K.; Conn, P. J.; Lindsley, C. W. Diverse Effects on M₁ Signaling and Adverse Effect Liability within a Series of M₁ Ago-PAMs. *ACS Chem. Neurosci.* **2017**, *8*, 866–883.

(15) Rook, J. M.; Berton, J. L.; Cho, H. P.; Gracia-Barrantes, P. M.; Moran, S. P.; Maksymetz, J. T.; Nance, K. D.; Dickerson, J. W.; Remke, D. H.; Chang, S.; Harp, J. M.; Blobaum, A. L.; Niswender, C. M.; Jones, C. K.; Stauffer, S. R.; Conn, P. J.; Lindsley, C. W. A novel M₁ PAM VU0486846 exerts efficacy in cognition models without displaying agonist activity or cholinergic toxicity. *ACS Chem. Neurosci.* **2018**, *9*, 2274–2285.

(16) Engers, J. L.; Childress, E. S.; Long, M. F.; Capstick, R. A.; Luscombe, V. B.; Cho, H. P.; Dickerson, J. W.; Rook, J. M.; Blobaum, A. L.; Niswender, C. M.; Conn, P. J.; Lindsley, C. W. VU6007477, a novel M₁ PAM based on a pyrrolo[2,3-*b*]pyridine carboxamide core devoid of cholinergic side effects. *ACS Med. Chem. Lett.* **2018**, *9*, 2641–2646.

(17) Sako, Y.; Kurimoto, E.; Mandai, T.; Suzuki, A.; Tanaka, M.; Suzuki, M.; Shimizu, Y.; Yamada, M.; Kiruma, H. TAK-071, a novel M₁ positive allosteric modulator with low cooperativity, improves cognitive function in rodents with few cholinergic side effects. *Neuropsychopharmacology* **2019**, *44*, 950–960.

(18) Yin, W.; Mamashli, F.; Buhl, F. M. D. L.; Buhl, D. L.; Khudyakov, P.; Khudyakov, P.; Volfson, D.; Volfson, D.; Martenyi, F.; Martenyi, F.; Gevorkyan, H.; Gevorkyan, H.; Rosen, L.; Rosen, L.; Simen, A. A. Safety, pharmacokinetics and quantitative EEG modulation of TAK-071, a novel muscarinic M₁ receptor positive allosteric modulator, in healthy subjects. *Br. J. Pharmacol.* **2022**, *88*, 600–612.

(19) Conley, A. C.; Key, A. P.; Blackford, J. U.; Rook, J. M.; Conn, P. J.; Lindsley, C. W.; Jones, C. K.; Newhouse, P. A. Cognitive performance effects following a single dose of the M₁ muscarinic positive allosteric modulator VU319. *Alzheimer's Dementia* **2020**, *16*, No. e045339.

(20) Conley, A. C.; Key, A. P.; Blackford, J. U.; Rook, J. M.; Conn, P. J.; Lindsley, C. W.; Jones, C. K.; Newhouse, P. A. Functional activity of the muscarinic positive allosteric modulator VU319 during a Phase 1 single ascending dose study. *Am. J. Geriatr. Psychiatry* **2021**, *29*, No. S43.

(21) See [Supporting Information](#) for full details.

(22) Storz, T.; Bartberger, M. D.; Sukits, S.; Wilde, C.; Soukup, T. The first practical and efficient one-pot synthesis of 6-substituted 7-azaindoles via a Reissert-Henze reaction. *Synthesis* **2008**, *2008*, 201–214.

(23) Hamilton, S. E.; Loose, M. D.; Qi, M.; Levey, A. I.; Hille, B.; McKnight, G. S.; Idzerda, R. L.; Nathanson, N. M. Disruption of the M₁ receptor gene ablates muscarinic receptor-dependent M current regulation and seizure activity in mice. *Proc. Natl. Acad. Sci. U.S.A.* **1997**, *94*, 13311–13316.

(24) Löscher, W.; Ferland, J.; Ferraro, T. N. The relevance of inter- and intrastain differences in mice and rats and their implications for models of seizures and epilepsy. *Epilepsy Behav.* **2017**, *73*, 214–235.